NIH Public Access
Author Manuscript
J Neurosci. Author manuscript; available in PMC 2010 January 8.

Published in final edited form as:
J Neurosci. 2009 July 8; 29(27): 8743–8751. doi:10.1523/JNEUROSCI.2294-09.2009.

Phosphorylation of Prion Protein at Serine 43 Induces Prion Protein Conformational Change

Paresa N. Giannopoulos[1], **Catherine Robertson**[2,3], **Julie Jodoin**[1,4], **Hemant Paudel**[1,4], **Stephanie A. Booth**[2,3], and **Andrea C. LeBlanc**[1,4]

[1] The Bloomfield Centre for Research in Aging, Lady Davis Institute for Medical Research, The Sir Mortimer B. Davis Jewish General Hospital, 3755 Ch. Côte Ste-Catherine, Montreal, Quebec, Canada H3T 1E2

[2] Molecular Pathobiology, National Microbiology Laboratory, Winnipeg, Manitoba, R3E 3R2, Canada

[3] Department of Medical Microbiology, University of Manitoba, Winnipeg, Manitoba, R3E 0J9, Canada

[4] Department of Neurology and Neurosurgery, McGill University, Montreal, Quebec, Canada, H3A 2T5

Abstract

The cause of the conformational change of normal cellular prion protein (PrP) into its disease-associated form is unknown. Post-translational modifications such as glycosylation, acetylation, S-nitrosylation, and phosphorylation are known to induce protein conformational changes. Here, we investigated if phosphorylation could induce PrP's conformational change because PrP contains several kinase motifs and has recently been found in the cytosol, where kinases generally reside. Neuronal cyclin-dependent kinase 5 (Cdk5) phosphorylated recombinant $PrP_{23\text{-}231}$ at serine 43 (S43) in an *in vitro* kinase assay. Cdk5-phosphorylated PrP became proteinase K resistant (PK^{RES}), formed Congo Red positive fibrils, and formed aggregates that were immunostained with anti-PrP and anti-phosphoPrP^{S43} (anti-pPrP^{S43}). pPrP^{S43} was detected in PrP/Cdk5/p25 co-transfected N2a cells. Roscovitine inhibition of Cdk5 activity or transfection of N2a cells with mutant PrP S43A eliminated the anti-pPrP^{S43} immunopositive protein. Alkaline phosphatase sensitive and proteinase K resistant pPrP^{S43} immunoreactivity was observed in scrapie-infected but not control-injected mice brains. These results raise the possibility that phosphorylation could represent a physiological mechanism of PrP conversion *in vivo*.

Key words (6)

cyclin-dependent kinase 5; conformation; phosphorylation; prion protein; scrapie; brain

Introduction

While it is widely accepted that conversion of normal cellular prion protein (PrP) into a proteinase K resistant (PK^{RES} or PrP^{RES}) aberrant conformational form is associated with transmissible spongiform encephalopathies, the underlying molecular mechanism of this

Corresponding author: Andréa LeBlanc, Ph.D. The Bloomfield Centre for Research in Aging, Lady Davis Institute for Medical Research, The Sir Mortimer B Davis Jewish, General Hospital, 3755 Ch. Côte Ste-Catherine, Montréal, Québec, Canada H3T 1E2 Canada, H3T 1E2. Tel: (514) 340-8260; Fax: (514) 340-8295; e-mail: andrea.leblanc@mcgill.ca.

NIH-PA Author Manuscript
NIH-PA Author Manuscript
NIH-PA Author Manuscript

NIH-PA Author Manuscript

conversion is not clear. The hypothesis that prion protein in the form of PrP^{RES} or PrP scrapie (PrP^{Sc}) is responsible for conversion of normal cellular PrP is well supported *in vivo* and *in vitro*. PrP^{Sc} seeded conversion is observed by infecting live animals (Prusiner, 1982; Caughey, 1993), specific cell lines (Race et al., 1987), and cell-free mammalian protein systems (Neary et al., 1991; Kocisco et al., 1994; Bessen et al., 1995; Saborio et al., 2001; Deleault et al., 2007).

Conversion is also observed in absence of PrP^{Sc} seed *in vivo*. Single point and insertional octapeptide repeat mutations of the Prnp gene generate PrP^{RES} (Monari et al., 1994; Tateishi and Kitamoto, 1995; Mastrianni et al., 2001; Piccardo et al., 2001; Grasbon-Frodl et al., 2004). Transgenic mice expressing the Gertsmann-Sträussler-Scheinker-associated PrP P101L mutation or PrP with a nine octapeptide repeat insertion result in a mild PrP^{RES} form of PrP (Hsiao et al., 1990; Chiesa et al., 1998). In the absence of a PrP mutation, endoplasmic reticulum associated degradation pathway (ERAD)-generated cytosolic PrP (CyPrP) becomes PK^{RES} in mouse N2a cells; however, this does not occur in human primary neurons or human neuroblastoma cell lines (Ma and Lindquist, 2002; Ma et al., 2002; Roucou et al., 2003).

In vitro, purified human, hamster or mouse $PrP_{90\text{-}231}$ or $PrP_{23\text{-}231}$ convert under acidic pH, mild denaturant conditions, treatment with 0.1% SDS and sonication, and protein misfolded cyclic amplification (PMCA) assay in the presence of RNA (Swietnicki et al., 1997; Jackson et al., 1999; Swietnicki et al., 2000; Deleault et al., 2003; Bocharova et al., 2006; Luhrs et al., 2006; Atarashi et al., 2007; Wang et al., 2007). Methionine oxidation, high pressure, Al^{3+} and Zn^{2+} also promote conversion of PrP and PrP fragments (Torrent et al., 2004; Breydo et al., 2005; Ricchelli et al., 2006). Conversion of PrP appears to first involve the formation of oligomers that evolve into fibrillar structures with time and give PK^{RES} fragments between 8-16 kDa (Jackson et al., 1999; Swietnicki et al., 2000; Xiong et al., 2001; Sokolowski et al., 2003; Breydo et al., 2005; Luhrs et al., 2006). Transmissibility of disease from PrP^{Sc}-free conversions has been observed only in two situations: by the injection of *E. Coli*-purified fibrillar $PrP_{89\text{-}231}$ in brains of transgenic mice overexpressing $PrP_{89\text{-}231}$ (Legname et al., 2004), and by infecting wild-type hamsters with purified mammalian PrP submitted to PMCA in the presence of poly-anions (Deleault et al., 2007).

Several anionic conditions such as anionic detergents, synthetic polyanions, RNA and low pH conditions favor the conformational change of PrP *in vitro* (Deleault et al., 2003; Supattapone, 2004; Deleault et al., 2005; Deleault et al., 2007; Geoghegan et al., 2007). Therefore, here, we considered the hypothesis that phosphorylation of PrP, which would also provide anionic conditions, could affect PrP conformation.

Material and Methods

Antibodies

The following commercially available antibodies were used: monoclonal 3F4 anti-$PrP^{109\text{-}112}$ (Kascsak et al., 1987), monoclonal 6H4 anti-$PrP^{144\text{-}156}$ (Prionics, Schlieren, Switzerland), monoclonal phosphoTyr (pTyr-100) (Cell Signaling Technology, Beverly, MA), HRP-conjugated goat anti-rabbit or anti-mouse IgG (Amersham/GE Healthcare, Arlington Heights, IL) and β-actin (Sigma Aldrich, Oakville, ON). The polyclonal R155 anti-$PrP^{36\text{-}56}$ was produced in our laboratory. The human PrP peptide Gly-phosphoSer-Pro-Gly-Gly-Asn-Arg-tyr-Pro terminating with an added Cys was synthesized, purified, conjugated to KLH and injected into rabbits by Sigma Genosys. ELISA performed by Genosys gave a titre of 1/25,000 for non-phosphopeptide and 1/500,000 for phosphopeptide after the first production bleed. The antiserum anti-$pPrP^{S43}$ was used at a titre of 1/100 for western blots and 1/250 for immunoprecipitation.

NIH-PA Author Manuscript

NIH-PA Author Manuscript

NIH-PA Author Manuscript

Site-directed mutagenesis of PrP and PrP purification

PrP S43A was generated by QuikChange site directed mutagenesis (Jodoin et al., 2007) with the forward primer 5′-CCGGGGCAGGGC**GCA**CCTGGAGGCAACC-3′ and the reverse primer 5′-GGTTGCCTCCAGG**TGC**GCCCTGCCCCGG-3′, from pBKSII-$PrP_{23\text{-}231}$ cDNA. The S43A mutation was confirmed by *Bgl*I digestion. PrP and PrP S43A were subcloned into the *BamH*I and *Xho*I sites of the pET-23b(+) vector (EMD Chemicals, Gibbstown, NJ) after PCR amplification with the forward primer 5′-ACGCGGATCCCAAGAAGCGCCCGAAGCCT-3′ and the reverse primer 5′-GCCGCTCGAGGCTCGATCCTCTCTGGTA-3′. The expression of C-terminally His tagged-PrP was induced in pET-23b(+)PrP or PrP S43A-transformed *E. Coli* BL21(DE3) pLysS (Stratagene, La Jolla, CA) with isopropyl-beta-D-thiogalactopyranoside and purified as described (Gilch et al., 2003). In addition, PrP S43A was introduced into pCep4β-PrP full-length (Bounhar et al., 2001) by QuikChange site directed mutagenesis.

Kinase Assay

One µl of Cdk5 kinase extracted from bovine brain (Paudel et al., 1993), 1.5 units of recombinant GST-Cdk5 with 2 units of GST-p25 (Calbiochem, La Jolla, CA), or 500 units of Casein kinase II (CKII; Biomol Research Laboratories, Plymouth Meeting, PA) were added to 0.45 µg/µl PrP (a generous gift from Dr. Witold Surewicz, Case Western Reserve University, Cleveland, OH) in kinase assay buffer containing 110.5 mM HEPES pH 7.2, 0.15 mM EDTA, 0.15 mM EGTA, 0.07 mM okadaic acid, 11.1 mM sodium fluoride, 11.1 mM $MgCl_2$, 1 µCi of (γ-^{32}P)-ATP (2 mCi/mL; Perkin-Elmer, Boston, MA), 2 mM ATP and EDTA-free protease inhibitor cocktail (Roche Applied Science, Laval, QC). The Cdk5 inhibitor, olomoucine (Biomol Research Laboratories, Plymouth Meeting, PA), was added at a concentration of 400 µM. The kinase reaction mix was incubated at 30°C for 4 hours, separated on 15% SDS-PAGE gels and visualized by overnight exposure for autoradiography or by western blotting with the monoclonal 3F4 antibody or the anti-$pPrP^{S43}$ antiserum. Immunoreactivity was detected with HRP-conjugated anti-mouse or anti-rabbit secondary antibodies and Immobilon™Western chemiluminescent HRP substrate reagents (Millipore, Mississauga, ON).

PK treatment of phosphorylated PrP

Various concentrations of PK (BioShop, Burlington, ON) in 50 mM Tris-HCl pH 7.5 ranging from 0 to 50 µg/mL were mixed with 2.3 µg of (γ-^{32}P)-phosphorylated or non-phosphorylated PrP in kinase reaction buffer containing freshly added 0.1 mM okadaic acid. The reaction mix was incubated at 4°C for 1 hr or at 37°C for 1 to 4 hours. The PK-treated PrP was analysed by autoradiography and western blot analyses as described above.

Effect of pPrP on non-phosphorylated PrP aggregation

Two µl (0.9 µg total PrP) of Cdk5-pPrP kinase assay or kinase assay without Cdk5 were added to 5.85 µg of PrP in a volume of 15 µl and incubated at 37°C for 0, 24, 48 and 96 hrs. After 96 hrs, 2 µl corresponding to 0.12 µg or 0.012 µg of the original kinase assays, were added to 5.85 µg of fresh PrP and incubated for 24hrs at 37°C (cycle 1) for serial propagation assays. The reaction was repeated for 6 cycles, transferring 2µl to fresh non-phosphorylated PrP at the end of each cycle. At the end of each cycle, 2 µl aliquots were also removed and added to 10 µl containing a final concentration of 0 (-PK) or 10 µg/ml PK (+PK), and digested at 37°C for 1 hr before submitting to a 3F4 western blot.

Transmission Electron Microscopy (TEM)

Kinase reactions were dialysed against 5 mM Tris-HCl pH 7.4 using the Slide-A-Lyzer® Mini Dialysis unit (Pierce, Rockford, Ill). Approximately 0.5 µl of the dialysed kinase reaction mix was deposited onto Formvar (Camemco Supplies, Quebec) coated copper grids for 2 minutes,

NIH-PA Author Manuscript
NIH-PA Author Manuscript
NIH-PA Author Manuscript

adsorbed with Whatman 1M filter paper, dried for 2 minutes, and stained with 4% uranyl acetate. Analyses of the samples were done with a FFI TECHNAI 12 120V TEM at the Facility for Electron Microscopy at McGill University. Controls consisted of non-phosphorylated PrP lacking Cdk5 in the reaction mix and Cdk5 in absence of PrP in the kinase reaction mix. Aging was done by incubating phosphorylated or non-phosphorylated dialysed PrP at 37°C for 16 days. Samples were frozen at -80°C until analysis by TEM.

Immuno-electron microscopy

Dialysed PrP or pPrP were placed on the grids as described above, blocked with a solution of 2% bovine serum albumin, 2% casein, and 0.5% ovalbumin (BCO) for 5 minutes. Anti-PrP antibodies were applied for 1 hr at room temperature at a dilution of 1/10 in BCO for 3F4 and anti-pPrP^{S43} and 1/20 for 6H4. After washes in Dulbecco's phosphate buffered saline (DPBS) and another 5 min blocking step in BCO, samples were incubated for 30 minutes with 1/20 anti-rabbit or anti-mouse IgG antibodies conjugated with 10 nm gold particles (Sigma, St-Louis, MO). After washing with DPBS, samples were stained with 4% uranyl acetate for 30 seconds to 1 minute. Controls included samples with no primary antibodies and immunostaining of $A\beta_{1-42}$ fibrils generated as described (Zhang et al., 2002). Co-immunostaining of PrP with 6H4 antibody and anti-pPrP^{S43} antiserum was detected with anti-mouse IgG conjugated to 5 nm gold (Sigma, St Louis, MO) and goat anti-Affinitypure Donkey anti-rabbit (H+L) conjugated to 18 nm gold particles (Jackson Immunoresearch, West Grove, PA).

Congo Red staining

Three µl of 10 µM dialysed PrP, Cdk5-phosphorylated PrP, PK digested Cdk5-phosphorylated PrP, fibrillar $A\beta_{1-42}$ and $A\beta_{42-1}$ (Zhang et al., 2002) and 0.05 µl of bovine brain purified Cdk5 were applied on glass slides and dried overnight at 4°C. Dried samples were stained for 2 hours with Congo Red solution (4 mM Congo Red, 50 mM NaCl, 80% EtOH) filtered on a 0.5 µm membrane. Samples were washed 4 times with 90% ethanol, dried and pictures were taken under polarized light microscopy.

Purification of phospho-proteins

Mouse neuroblastoma Neuro2a (N2a) cells (ATCC) were cultured in MEM containing 10% fetal bovine serum (HyClone, Logan, UT) and transfected with pCep4β-PrP, pCep4β-PrP/pcDNA3.1-Cdk5/pcDNA3.1-p25, or pCep4β-PrP S43A/pcDNA3.1-Cdk5/pcDNA3.1-p25 (Bounhar et al., 2001; Li et al., 2007) using Lipofectamine^{2000} reagent (Invitrogen, Burlington, ON). Cells were maintained in culture in the presence of 100 nM okadaic acid (BioShop, Burlington, ON). For the roscovitine treatments, 10 µM roscovitine (Biomol Research Laboratories, Plymouth Meeting, PA) was added 24 hrs after the transfection and cells were maintained in culture for an additional 24 hrs. Proteins were collected 48 hrs after the transfection and phospho-proteins purified with the PhosphoPurification kit according to the manufacturer's instructions (Qiagen, Mississauga, ON).

Immunohistochemistry on mice brains

C57BL6 mice were intracerebrally inoculated with 20µl of a 1% brain homogenate from mice infected with the 22A strain of scrapie (TSE Resource Centre, Compton U.K.) The animals were sacrificed at onset of clinical symptoms and the whole brains were fixed in 10% formalin, then processed and embedded in paraffin wax. Brains of age matched, mock-infected mice were collected as controls. Four micron sections were deparaffinized, rehydrated, autoclaved in sodium citrate antigen retrieval buffer (10mM sodium citrate, 0.05% Tween 20, pH 6.0) at 121°C 30 min, washed with TBS-T (0.1 % Triton X-100, 20 mM Tris, 150 mM NaCl, pH 7.5), and blocked with Power Block Universal blocking reagent (Inter Medico, ON). The anti-

NIH-PA Author Manuscript

$pPrP^{S43}$ antiserum (1/200) was incubated overnight at 4°C followed by washing in TBS-T and incubating with UltraVision One AP polymer according to the UltraVision ONE Detection System protocol (Thermo Fisher Scientific, CA). The tissue sections were counterstained with Haematoxylin. When indicated, before the first antibody incubation, the sections were treated at 37°C for 1 hr with 150 U/ml alkaline phosphatase (Fermentas, ON) or 15 min with a 1:50 dilution of ready to use proteinase K (Dako Canada Inc, ON). For the adsorption of the anti-$pPrP^{S43}$ antiserum, diluted antiserum (1/200) was incubated overnight at 4°C with 20 μg/ml $pPrP^{S43}$ peptide, centrifuged, and the supernatant was used as adsorbed antiserum.

Results

Cdk5 phosphorylation of PrP_{23-231}

Several kinase motifs are highly conserved in PrP (Table I). We focussed on Cdk5 because it is an abundant neuronal kinase involved in neurodegeneration and neurons are the cell type most affected in prion diseases. Cdk5 phosphorylates serine-proline (SP) motifs. Prion protein has two SP phosphorylation motifs: one in the N-terminus part of the mature protein at amino acid Ser43/Pro44 and one in the GPI-anchor signal peptide at S237/P238 (Table I). *In vitro* phosphorylation of PrP_{23-231} with Cdk5 showed intense phosphorylation of the full-length and a fragment of PrP_{23-231}, similar to Cdk5-phosphorylation of the known Cdk5 substrate, Tau protein (Fig. 1A&B). The Cdk5 inhibitor, olomoucine, largely inhibited PrP phosphorylation (Fig. 1C). To determine if Cdk5 phosphorylates PrP at S43, we mutated S43 to A43 in PrP_{23-231}. The PrP S43A was labeled poorly compared to the wild type protein (Fig. 1D).

We then generated an antiserum against pPrP at S43 (anti-$pPrP^{S43}$). The anti-$pPrP^{S43}$ recognized the Cdk5-phosphorylated PrP (pPrP), but not the non-phosphorylated PrP (Fig. 1E). Anti-$pPrP^{S43}$ immunoprecipitated Cdk5-phosphorylated PrP, but not the non-phosphorylated PrP, indicating that this antiserum recognized native pPrP (Fig. 1F). In contrast, R155 (anti-PrP^{36-56}) immunoprecipitated both pPrP and PrP. The anti-$pPrP^{S43}$ did not recognize Cdk5-phosphorylated mutant PrP S43A thus confirming that S43 is the site of phosphorylation (Fig. 1G). Together, these results indicate that S43 is a major Cdk5 phosphorylation site in PrP.

Cdk5-phosphorylated PrP converts to a PK^{RES} form

To determine if PrP phosphorylation induces PK^{RES}, we submitted the ^{32}P-phosphorylated PrP to increasing amounts of PK. A ^{32}P-pPrP peptide of approximately 10 kDa robustly resisted a one-hour treatment of 10 μg/ml PK at 4°C or 37°C (Fig. 2A) and 4 hours of 50 μg/ml PK digestion at 37°C (Fig. 2B). These results indicate that the pPrP has either undergone a conformational change or developed aggregates that resist PK digestion.

To assess if phosphorylation at other amino acid residues can also induce PK^{RES} of PrP, PrP was phosphorylated with CKII, known to phosphorylate bovine PrP at Ser154 (equivalent to S143 in humans) (Negro et al., 2000). However, CKII-phosphorylated human PrP did not become PK^{RES} (Fig. 2C). These results indicate that Cdk5-phosphorylated PrP specifically becomes PK^{RES}.

Cdk5-phosphorylated PrP induces the aggregation of non-phosphorylated PrP

To determine if non-^{32}P-labeled PrP in the reaction mixture was also resistant to PK, the Cdk5-phosphorylated PrP was immunoblotted (Fig. 3A). The non-phosphorylated PrP was completely degraded by PK, but the Cdk5-phosphorylated PrP was not. The 3F4 antibody detected PK^{RES} 25 kDa full-length, the 16 kDa and 18 kDa co-purified PrP fragments, and faintly the 10 kDa radiolabeled PrP^{RES} fragment. Together, these results show that firstly the PK^{RES} radiolabeled 10 kDa fragment contains the phosphorylated S43, and secondly that non-phosphorylated 25 kDa full-length PrP can become PK^{RES} in the kinase assay. The 16 and 18

NIH-PA Author Manuscript

kDa non-radiolabeled PK^{RES} fragments either represent pPrP after the proteolytic cleavage of PrP's N-terminus containing the pS43 epitope or non-phosphorylated PK^{RES} PrP fragments. Seeding PrP from the Cdk5 kinase assay generated a small amount of PK^{RES} non-phosphorylated full length PrP and PrP fragments after 24 hrs of incubation, whereas seeding PrP from the kinase assay lacking Cdk5 did not (Fig. 3B). Furthermore, a longer exposure demonstrated an increase of the 10 kDa PrP fragment at 24 and 48 hrs. At 48 and 96 hrs of incubation, aggregated PrP representing oligomers of varying sizes were also generated as evidenced by the smear at the top of the western blot (Fig. 3B).

To assess if pPrP can convert non-phosphorylated PrP into a PK^{RES} protein in a serial propagation assay, 2 μl or 0.2 μl of the 96 hr reaction mix in Fig. 3B, was incubated 24 hrs with fresh non-phosphorylated PrP before testing for PK^{RES} and this was repeated 6 times (cycles), each time seeding fresh non-phosphorylated PrP with 2 μl of the incubation mix at the end of the 24 hr incubation period. Increasing amounts of PK^{RES} full length PrP and PrP fragments were obtained from the Cdk5-containing kinase assay seeded PrP mix after 3 cycles, but not from the non Cdk5-containing kinase assay (Fig. 3C). However, no further amplification of the 10 kDa PK^{RES} PrP fragment was obtained. Seeding with 0.2 μl of the Cdk5-kinase assay also resulted in PK^{RES} PrP after 6 cycles. These results indicate that pPrP enhances non-phophorylated PrP aggregation but not conversion.

Cdk5-phosphorylated PrP forms aggregates and fibrils

To evaluate the structural state of PrP after phosphorylation, we analysed PrP and pPrP by transmission electron microscopy. Globular aggregates were detected in the pPrP and much less abundantly in the non-phosphorylated PrP reaction mixture (Fig. 4). The Cdk5 alone did not contain these structures (not shown). The globular structures had various appearances: some were monomeric whereas others were aggregated. Immunodecoration with the anti-PrP 6H4 and 3F4 antibodies (3F4 not shown) and anti-$pPrP^{S43}$ antiserum confirmed that PrP and pPrP were present in these globular structures (Fig. 4A&B). Both epitopes co-localized but did not overlap in these globular aggregates (Fig. 4C). No immunoreactivity was observed in absence of primary antibodies (not shown). These two antibodies did not recognize $A\beta_{1-42}$ fibrils thus indicating specificity (Fig. 4D). The 6H4 antibody recognized non-phosphorylated PrP (Fig. 4E), but anti-$pPrP^{S43}$ did not (Fig. 4F).

In addition, large fibrils were detected in transmission electron micrographs of pPrP (Fig. 5A). These increased in abundance and diversity with an incubation of the Cdk5-phosphorylated PrP at 37°C for 16 days (Fig. 5B), a method commonly utilized to enhance fibrillization of peptides. The globular aggregates also seem to become more compacted with time (Fig. 5C). In contrast, non-phosphorylated PrP remained amorphous with time of incubation (Fig. 5D).

To determine if pPrP had taken an amyloid conformation, we conducted Congo Red staining (Fig. 5E). Whereas neither the PrP nor the Cdk5 preparation stained with Congo Red, Cdk5-pPrP displayed fibril-like structures with the expected apple green birefringence appearance under polarized light. These structures resembled those observed with the fibrillar amyloid β peptide 1-42 ($A\beta_{1-42}$). The reverse control peptide $A\beta_{42-1}$ was negative, as expected. Treatment of the proteins with PK did not remove these Congo Red positive structures in Cdk5-phosphorylated PrP. Together, these results show that phosphorylation of PrP induces a conformational change in PrP.

Phosphorylated PrP is detected in PrP/Cdk5/p25 co-transfected N2a cells

To examine if PrP can be phosphorylated in live cells, we transfected mouse neuroblastoma N2a cells with wild type human PrP, Cdk5 and p25 cDNAs and isolated phospho-proteins from total cellular protein extracts. PrP was expressed at high levels and most was recuperated in

NIH-PA Author Manuscript NIH-PA Author Manuscript NIH-PA Author Manuscript

the flow-through of the phospho-column (Fig. 6A). Four 3F4-positive 25-30 kDa proteins were recovered in fractions 2-4 with most of the protein eluting in fraction 3 (F3). Immunoblotting with an anti-phospho-tyrosine antiserum (pTyr) confirmed that F3 contained most of the phospho-proteins. The anti-pPrP^{S43} antiserum recognized one of the four 3F4 positive proteins in F3. To determine if Cdk5 phosphorylated any of these pPrP, we treated the transfected cells with the Cdk5 inhibitor, roscovitine. Three 3F4 positive PrP proteins were observed in the phospho fraction (Fig. 6B). Furthermore, transfection of N2a cells with full-length PrP S43A rather than wild type PrP or wild type PrP in absence of Cdk5/p25, also yielded only three proteins (Fig. 6C&D). As expected, no 3F4 immunoreactivity was detected in the phospho-proteins purified from untransfected N2a cells (Fig. 6E). These results indicate that PrP is phosphorylated at S43 by a roscovitine sensitive kinase. In addition, the results show additional Cdk5-independent PrP phosphorylation.

Alkaline phosphatase sensitive and proteinase K resistant pPrP^{S43} immunoreactivity in scrapie infected mice brains

To assess if pPrP^{S43} could be part of the pathogenic process in scrapie infections, we immunostained coronal sections of mock-infected or 22A scrapie-infected mouse brains with the anti-pPrP^{S43}antiserum (Fig. 7). No immunoreactivity was detected in the mock-infected brains. However, widespread immunostaining was detected in the 22A-infected brains, especially in the medulla and thalamus region, which are the regions normally affected by the 22A strain. In contrast, no immunoreactivity was detected in the hypothalamus, which shows relatively little prion-associated pathology in this model. The pPrP^{S43} immunoreactivity was mostly located in diffuse deposits of PrP^{Sc}, and in the cytoplasm of neurons (Fig. 8). Occasionally strong staining was also detected in the nucleus of some cells (Fig. 8). The anti-pPrP^{S43} immunoreactivity was eliminated with a pre-treatment of the tissue sections with alkaline phosphatase thus confirming detection of the phospho-epitope by the antiserum (Fig. 7). In contrast, the immunoreactivity to pPrP^{S43} was preserved in PK-treated tissue sections indicating that pPrP is part of the pathogenic PrP. Immunoreactivity was completely absorbed with pPrP^{S43}peptide and was not detected in the absence of primary antiserum. These results indicate that PK^{RES} pPrP^{S43} is also present in infectious PrP diseases

Discussion

Here, we show that neuronal Cdk5 phosphorylates PrP at amino acid residue S43 and that this phosphorylation results in the conversion of PrP. That phosphorylated PrP is converted into a conformationally different form is evidenced by (1) PK^{RES} of a 10 kDa phosphorylated PrP fragment, (2) the transformation of the phosphorylated PrP into amyloid structures that project an apple green birefringence under polarized light, and (3) the formation in time of fibrils detected by transmission electron microscopy. The conversion of PrP seems specific to Cdk5 phosphorylation at S43 since phosphorylation by CKII at S143 does not generate phosphorylated PK^{RES} fragments of PrP.

The converted pPrP does not appear to have the ability to convert non-phosphorylated PrP into a 10 kDa PK^{RES} PrP fragment *in vitro*. While a small amount of PK^{RES} 10 kDa PrP fragment is detected after 24 and 48 hours of incubation of non-phosphorylated PrP seeded with 6 fold less of the pPrP mix, it does not further amplify in time. Furthermore, consecutive cycles of dilutions and incubations did not amplify the 10 kDa fragment. However, as discussed below, the pPrP has the ability to enhance non-phosphorylated PrP aggregation. The lack of amplification of converted PrP in these experiments is consistent with the inability to convert bacterially purified PrP with scrapie prions *in vitro* (Deleault et al., 2005). Nevertheless, the conversion of PrP by Cdk5 phosphorylation provides a physiological molecular mechanism that could explain conversion *in vivo*. Alkaline phosphatase sensitive and proteinase K resistant

NIH-PA Author Manuscript

pPrP^{S43} immunoreactivity is observed in the expected strain-specific pattern of PrP^{Sc} deposition in 22A scrapie-infected mice brains, indicating that phosphorylation of PrP occurs in pathological conditions. Phosphorylation is a well-known mechanism of enzymatic activation through the induction of protein conformational change. Phosphorylation either changes the tertiary structure of globular proteins or has a direct effect on the dihedral backbone of the protein (Tholey et al., 1999). Since the prion protein N-terminus is highly flexible (Donne et al., 1997; Zahn et al., 2000), it is possible that the phosphorylation at S43 provides a higher ordered structure or allows electrostatic interactions with other amino acids intra- or inter-molecularly to generate PK resistance.

While we could not observe an amplification of the 10 kDa pPrP fragment in non-phosphorylated PrP, the phosphorylation of PrP induced PK^{RES} of non-phosphorylated PrP *in vitro*. These PK^{RES} forms of PrP are likely produced by aggregation because of the co-existence, but not overlap, of the pPrP^{S43} and 6H4 epitopes in PrP protein aggregates detected by electron microscopy. Furthermore, pPrP promotes PK^{RES} of full length and 16 or 18 kDa fragments of PrP. Because the size of the non-phosphorylated PrP does not shift with PK treatment, these results infer that pPrP induces non-phosphorylated PrP aggregation, rather than conversion. This assumption is further supported by a time-dependent increase in high molecular weight PrP aggregates and full length PrP when recombinant non-phosphorylated PrP is seeded with 6 fold less pPrP reaction mix and incubated at 37°C. Furthermore, serial propagation of pPrP, originally diluted 50 or 500 fold from the kinase assay, into recombinant non-phosphorylated PrP, resulted in the production of PK^{RES} PrP after 3 and 6 cycles of incubation, respectively. Therefore, pPrP enhances aggregation rather than converts non-phosphorylated PrP. However, we cannot exclude the possibility that over a very long period of time, the pPrP may actually convert non-phosphorylated PrP.

NIH-PA Author Manuscript

In transmissible prion diseases, PrP conversion is thought to occur either by template-directed conversion of PrP or by seeded nucleation (reviewed by (Aguzzi and Polymenidou, 2004)). In template-directed conversion, the converted PrP molecule recruits and changes the conformation of normal PrP. In seeded nucleation, the conformationally abnormal protein recruits additional abnormal proteins to form a scaffold of abnormal proteins. However, the mechanism involved in the initial conversion of PrP is unknown. Phosphorylation may represent a physiological event that can originally convert PrP. The negative charges of the phosphate group may act in a manner similar to other anionic molecules such as RNA, anionic lipid bicelles, low pH conditions, and synthetic poly-anions that have been shown to induce PrP conversion *in vitro* (Deleault et al., 2003; Supattapone, 2004; Deleault et al., 2005; Deleault et al., 2007; Geoghegan et al., 2007).

We cannot affirm that the pPrP^{S43} epitope *in vivo* is the result of only Cdk5 phosphorylation because other kinases such as MAPK and GSK3β may also phosphorylate this residue. However, given that Cdk5 is known as a neuronal kinase associated with several pathological events in neurodegenerative diseases, including translocation from the nuclei to the cytosol (Zhang et al., 2008), our results suggest neuronal specificity to this modification of PrP. In addition, PrP is phosphorylated at sites other than S43 and independently from Cdk5 in N2a cells. The three additional pPrP forms observed in N2a cells could represent alternative phosphorylation by other kinases, or phosphorylated PrP that is differentially glycosylated or post-translationally modified. Others have reported *in vitro* phosphorylation of bovine PrP with protein kinase C, CKII, and two tyrosine kinases, Lyn and c-Fgr (Negro et al., 2000). However, the effect of phosphorylation on PrP conformation was not reported. We have shown here that CKII phosphorylation of PrP does not induce PK^{RES}. Further investigations into the role of phosphorylation by the various kinases in either the normal PrP function or in the pathological PrP disease mechanism are warranted by these initial findings.

NIH-PA Author Manuscript

NIH-PA Author Manuscript

NIH-PA Author Manuscript

NIH-PA Author Manuscript

Phosphorylation-dependent conversion of non-enzyme proteins may be a general mechanism associated with neurodegenerative diseases. Phosphorylation is associated with conversion of alpha-synuclein and Tau protein in Parkinson disease and Alzheimer disease, respectively (Okochi et al., 2000; Fujiwara et al., 2002). Phosphorylated alpha-synuclein becomes PK^{RES} and misfolded in disease (Neumann et al., 2002) and phosphorylated Tau resists calpain- and thrombin-mediated degradation (Litersky and Johnson, 1992; Arai et al., 2005). However, there is no direct evidence that phosphorylation induces a conformational change of these proteins. Our results with recombinant prion protein show that Cdk5-dependent phosphorylation is directly responsible for the conversion of prion protein. These results raise the possibility that other cytosolic proteins undergo a phosphorylation-dependent conformational change in disease.

In summary, we showed in this study an entirely physiological condition that could explain PrP conversion in prion diseases. This work has two important implications. First, the phosphorylated PrP epitope at S43 may be an excellent candidate for diagnostic purposes. Second, if phosphorylation of PrP at S43 is involved in the pathophysiology of disease, inhibitors of SP-directed kinases could be used as a therapeutic intervention against prion diseases.

Acknowledgments

The authors wish to thank Dr. Witold Surewicz (Case Western Reserve University, OH, USA) for providing recombinant PrP, Dr. Hajatollah Vali (Dept. Anatomy and Cell Biology, McGill U.) for helping with the electron microscopy work. This work was supported by the National Institutes of Health 1RO1 NS40431, Canadian Institutes for Health Research MOP-49594 and Fonds de recherche en Santé du Québec to ALB and the Public Health Agency of Canada, the Canadian Biotechnology Strategy Fund: Genomics Initiative for Government Laboratories and Public Health Service and Prionet Canada to SAB.

References

Aguzzi A, Polymenidou M. Mammalian prion biology: one century of evolving concepts. Cell 2004;116:313–327. [PubMed: 14744440]

Arai T, Guo JP, McGeer PL. Proteolysis of non-phosphorylated and phosphorylated tau by thrombin. J Biol Chem 2005;280:5145–5153. [PubMed: 15542598]

Atarashi R, Moore RA, Sim VL, Hughson AG, Dorward DW, Onwubiko HA, Priola SA, Caughey B. Ultrasensitive detection of scrapie prion protein using seeded conversion of recombinant prion protein. Nat Methods 2007;4:645–650. [PubMed: 17643109]

Bessen RA, Kocisko DA, Raymond GJ, Nandan S, Lansbury PT, Caughey B. Non-genetic propagation of strain-specific properties of scrapie prion protein. Nature 1995;375:698–700. [PubMed: 7791905]

Bocharova OV, Makarava N, Breydo L, Anderson M, Salnikov VV, Baskakov IV. Annealing prion protein amyloid fibrils at high temperature results in extension of a proteinase K-resistant core. J Biol Chem 2006;281:2373–2379. [PubMed: 16314415]

Bounhar Y, Zhang Y, Goodyer CG, LeBlanc A. Prion protein protects human neurons against Bax-mediated apoptosis. J Biol Chem 2001;276:39145–39149. [PubMed: 11522774]

Breydo L, Bocharova OV, Makarava N, Salnikov VV, Anderson M, Baskakov IV. Methionine oxidation interferes with conversion of the prion protein into the fibrillar proteinase K-resistant conformation. Biochemistry 2005;44:15534–15543. [PubMed: 16300402]

Caughey B. Scrapie associated PrP accumulation and its prevention: insights from cell culture. Br Med Bull 1993;49:860–872. [PubMed: 8137133]

Chiesa R, Piccardo P, Ghetti B, Harris DA. Neurological illness in transgenic mice expressing a prion protein with an insertional mutation. Neuron 1998;21:1339–1351. [PubMed: 9883727]

Deleault NR, Lucassen RW, Supattapone S. RNA molecules stimulate prion protein conversion. Nature 2003;425:717–720. [PubMed: 14562104]

Deleault NR, Harris BT, Rees JR, Supattapone S. Formation of native prions from minimal components in vitro. Proc Natl Acad Sci U S A 2007;104:9741–9746. [PubMed: 17535913]

NIH-PA Author Manuscript NIH-PA Author Manuscript NIH-PA Author Manuscript

Deleault NR, Geoghegan JC, Nishina K, Kascsak R, Williamson RA, Supattapone S. Protease-resistant prion protein amplification reconstituted with partially purified substrates and synthetic polyanions. J Biol Chem 2005;280:26873–26879. [PubMed: 15917229]

Donne DG, Viles JH, Groth D, Mehlhorn I, James TL, Cohen FE, Prusiner SB, Wright PE, Dyson HJ. Structure of the recombinant full-length hamster prion protein PrP(29-231): the N terminus is highly flexible. Proc Natl Acad Sci U S A 1997;94:13452–13457. [PubMed: 9391046]

Fujiwara H, Hasegawa M, Dohmae N, Kawashima A, Masliah E, Goldberg MS, Shen J, Takio K, Iwatsubo T. alpha-Synuclein is phosphorylated in synucleinopathy lesions. Nat Cell Biol 2002;4:160–164. [PubMed: 11813001]

Geoghegan JC, Valdes PA, Orem NR, Deleault NR, Williamson RA, Harris BT, Supattapone S. Selective incorporation of polyanionic molecules into hamster prions. J Biol Chem 2007;282:36341–36353. [PubMed: 17940287]

Gilch S, Wopfner F, Renner-Muller I, Kremmer E, Bauer C, Wolf E, Brem G, Groschup MH, Schatzl HM. Polyclonal anti-PrP auto-antibodies induced with dimeric PrP interfere efficiently with PrPSc propagation in prion-infected cells. J Biol Chem 2003;278:18524–18531. [PubMed: 12637572]

Grasbon-Frodl E, Lorenz H, Mann U, Nitsch RM, Windl O, Kretzschmar HA. Loss of glycosylation associated with the T183A mutation in human prion disease. Acta Neuropathol 2004;108:476–484. [PubMed: 15558291]

Hsiao KK, Scott M, Foster D, Groth DF, DeArmond SJ, Prusiner SB. Spontaneous neurodegeneration in transgenic mice with mutant prion protein. Science 1990;250:1587–1590. [PubMed: 1980379]

Jackson GS, Hosszu LL, Power A, Hill AF, Kenney J, Saibil H, Craven CJ, Waltho JP, Clarke AR, Collinge J. Reversible conversion of monomeric human prion protein between native and fibrilogenic conformations. Science 1999;283:1935–1937. [PubMed: 10082469]

Jodoin J, Laroche-Pierre S, Goodyer CG, LeBlanc AC. Defective retrotranslocation causes loss of anti-Bax function in human familial prion protein mutants. J Neurosci 2007;27:5081–5091. [PubMed: 17494694]

Kascsak RJ, Rubenstein R, Merz PA, Tonna-DeMasi M, Fersko R, Carp RI, Wisniewski HM, Diringer H. Mouse polyclonal and monoclonal antibody to scrapie-associated fibril proteins. J Virol 1987;61:3688–3693. [PubMed: 2446004]

Kocisco DA, Come JH, Priola SA, Chesebro B, Raymond GJ, Lansbury PT, Caughey B. Cell-free formation of protease-resistant prion protein. Nature 1994;370:471–474. [PubMed: 7913989]

Legname G, Baskakov IV, Nguyen HO, Riesner D, Cohen FE, DeArmond SJ, Prusiner SB. Synthetic mammalian prions. Science 2004;305:673–676. [PubMed: 15286374]

Li T, Chalifour LE, Paudel HK. Phosphorylation of protein phosphatase 1 by cyclin-dependent protein kinase 5 during nerve growth factor-induced PC12 cell differentiation. J Biol Chem 2007;282:6619–6628. [PubMed: 17202132]

Litersky JM, Johnson GV. Phosphorylation by cAMP-dependent protein kinase inhibits the degradation of tau by calpain. J Biol Chem 1992;267:1563–1568. [PubMed: 1730702]

Luhrs T, Zahn R, Wuthrich K. Amyloid formation by recombinant full-length prion proteins in phospholipid bicelle solutions. J Mol Biol 2006;357:833–841. [PubMed: 16466741]

Ma J, Lindquist S. Conversion of PrP to a self-perpetuating PrPSc-like conformation in the cytosol. Science 2002;298:1785–1788. [PubMed: 12386336]

Ma J, Wollmann R, Lindquist S. Neurotoxicity and neurodegeneration when PrP accumulates in the cytosol. Science 2002;298:1781–1785. [PubMed: 12386337]

Mastrianni JA, Capellari S, Telling GC, Han D, Bosque P, Prusiner SB, DeArmond SJ. Inherited prion disease caused by the V210I mutation: transmission to transgenic mice. Neurology 2001;57:2198–2205. [PubMed: 11756597]

Monari L, Chen SG, Brown P, Parchi P, Petersen RB, Mikol J, Gray F, Cortelli P, Montagna P, Ghetti B, et al. Fatal familial insomnia and familial Creutzfeldt-Jakob disease: different prion proteins determined by a DNA polymorphism. Proc Natl Acad Sci U S A 1994;91:2839–2842. [PubMed: 7908444]

Neary K, Caughey B, Ernst D, Race RE, Chesebro B. Protease Sensitivity and Nuclease Resistance of the Scrapie Agent Propagated Invitro in Neuroblastoma Cells. J Virol 1991;65:1031–1034. [PubMed: 1846182]

NIH-PA Author Manuscript

NIH-PA Author Manuscript

NIH-PA Author Manuscript

Negro A, Meggio F, Bertoli A, Battistutta R, Sorgato MC, Pinna LA. Susceptibility of the prion protein to enzymic phosphorylation. Biochem Biophys Res Commun 2000;271:337–341. [PubMed: 10799298]

Neumann M, Kahle PJ, Giasson BI, Ozmen L, Borroni E, Spooren W, Muller V, Odoy S, Fujiwara H, Hasegawa M, Iwatsubo T, Trojanowski JQ, Kretzschmar HA, Haass C. Misfolded proteinase K-resistant hyperphosphorylated alpha-synuclein in aged transgenic mice with locomotor deterioration and in human alpha-synucleinopathies. J Clin Invest 2002;110:1429–1439. [PubMed: 12438441]

Okochi M, Walter J, Koyama A, Nakajo S, Baba M, Iwatsubo T, Meijer L, Kahle PJ, Haass C. Constitutive phosphorylation of the Parkinson's disease associated alpha-synuclein. J Biol Chem 2000;275:390–397. [PubMed: 10617630]

Paudel HK, Lew J, Ali Z, Wang JH. Brain proline-directed protein kinase phosphorylates tau on sites that are abnormally phosphorylated in tau associated with Alzheimer's paired helical filaments. J Biol Chem 1993;268:23512–23518. [PubMed: 8226879]

Piccardo P, Liepnieks JJ, William A, Dlouhy SR, Farlow MR, Young K, Nochlin D, Bird TD, Nixon RR, Ball MJ, DeCarli C, Bugiani O, Tagliavini F, Benson MD, Ghetti B. Prion proteins with different conformations accumulate in Gerstmann-Straussler-Scheinker disease caused by A117V and F198S mutations. Am J Pathol 2001;158:2201–2207. [PubMed: 11395398]

Prusiner SB. Novel proteinaceous infectious particles cause scrapie. Science 1982;216:136–144. [PubMed: 6801762]

Race RE, Fadness LH, Chesebro B. Characterization of scrapie infection in mouse neuroblastoma cells. J Gen Virol 1987;68(Pt 5):1391–1399. [PubMed: 3106566]

Ricchelli F, Buggio R, Drago D, Salmona M, Forloni G, Negro A, Tognon G, Zatta P. Aggregation/fibrillogenesis of recombinant human prion protein and Gerstmann-Straussler-Scheinker disease peptides in the presence of metal ions. Biochemistry 2006;45:6724–6732. [PubMed: 16716083]

Roucou X, Guo Q, Zhang Y, Goodyer CG, LeBlanc AC. Cytosolic prion protein is not toxic and protects against Bax-mediated cell death in human primary neurons. J Biol Chem 2003;278:40877–40881. [PubMed: 12917444]

Saborio GP, Permanne B, Soto C. Sensitive detection of pathological prion protein by cyclic amplification of protein misfolding. Nature 2001;411:810–813. [PubMed: 11459061]

Sokolowski F, Modler AJ, Masuch R, Zirwer D, Baier M, Lutsch G, Moss DA, Gast K, Naumann D. Formation of critical oligomers is a key event during conformational transition of recombinant syrian hamster prion protein. J Biol Chem 2003;278:40481–40492. [PubMed: 12917432]

Supattapone S. Prion protein conversion in vitro. J Mol Med 2004;82:348–356. [PubMed: 15014886]

Swietnicki W, Petersen R, Gambetti P, Surewicz WK. pH-dependent stability and conformation of the recombinant human prion protein PrP(90-231). J Biol Chem 1997;272:27517–27520. [PubMed: 9346881]

Swietnicki W, Morillas M, Chen SG, Gambetti P, Surewicz WK. Aggregation and fibrillization of the recombinant human prion protein huPrP90-231. Biochemistry 2000;39:424–431. [PubMed: 10631004]

Tateishi J, Kitamoto T. Inherited prion diseases and transmission to rodents. Brain Pathol 1995;5:53–59. [PubMed: 7767491]

Tholey A, Lindemann A, Kinzel V, Reed J. Direct effects of phosphorylation on the preferred backbone conformation of peptides: a nuclear magnetic resonance study. Biophys J 1999;76:76–87. [PubMed: 9876124]

Torrent J, Marchal S, Tortora P, Lange R, Balny C. High pressure, an alternative approach to understand protein misfolding diseases. Cell Mol Biol (Noisy-le-grand) 2004;50:377–385. [PubMed: 15529748]

Wang F, Yang F, Hu Y, Wang X, Wang X, Jin C, Ma J. Lipid interaction converts prion protein to a PrPSc-like proteinase K-resistant conformation under physiological conditions. Biochemistry 2007;46:7045–7053. [PubMed: 17503780]

Xiong LW, Raymond LD, Hayes SF, Raymond GJ, Caughey B. Conformational change, aggregation and fibril formation induced by detergent treatments of cellular prion protein. J Neurochem 2001;79:669–678. [PubMed: 11701770]

NIH-PA Author Manuscript

NIH-PA Author Manuscript

NIH-PA Author Manuscript

Zahn R, Liu A, Luhrs T, Riek R, von Schroetter C, Lopez Garcia F, Billeter M, Calzolai L, Wider G, Wuthrich K. NMR solution structure of the human prion protein. Proc Natl Acad Sci U S A 2000;97:145–150. [PubMed: 10618385]

Zhang J, Cicero SA, Wang L, Romito-Digiacomo RR, Yang Y, Herrup K. Nuclear localization of Cdk5 is a key determinant in the postmitotic state of neurons. Proc Natl Acad Sci U S A 2008;105:8772–8777. [PubMed: 18550843]

Zhang Y, McLaughlin R, Goodyer C, LeBlanc A. Selective cytotoxicity of intracellular amyloid beta peptide1-42 through p53 and Bax in cultured primary human neurons. J Cell Biol 2002;156:519–529. [PubMed: 11815632]

NIH-PA Author Manuscript
NIH-PA Author Manuscript
NIH-PA Author Manuscript

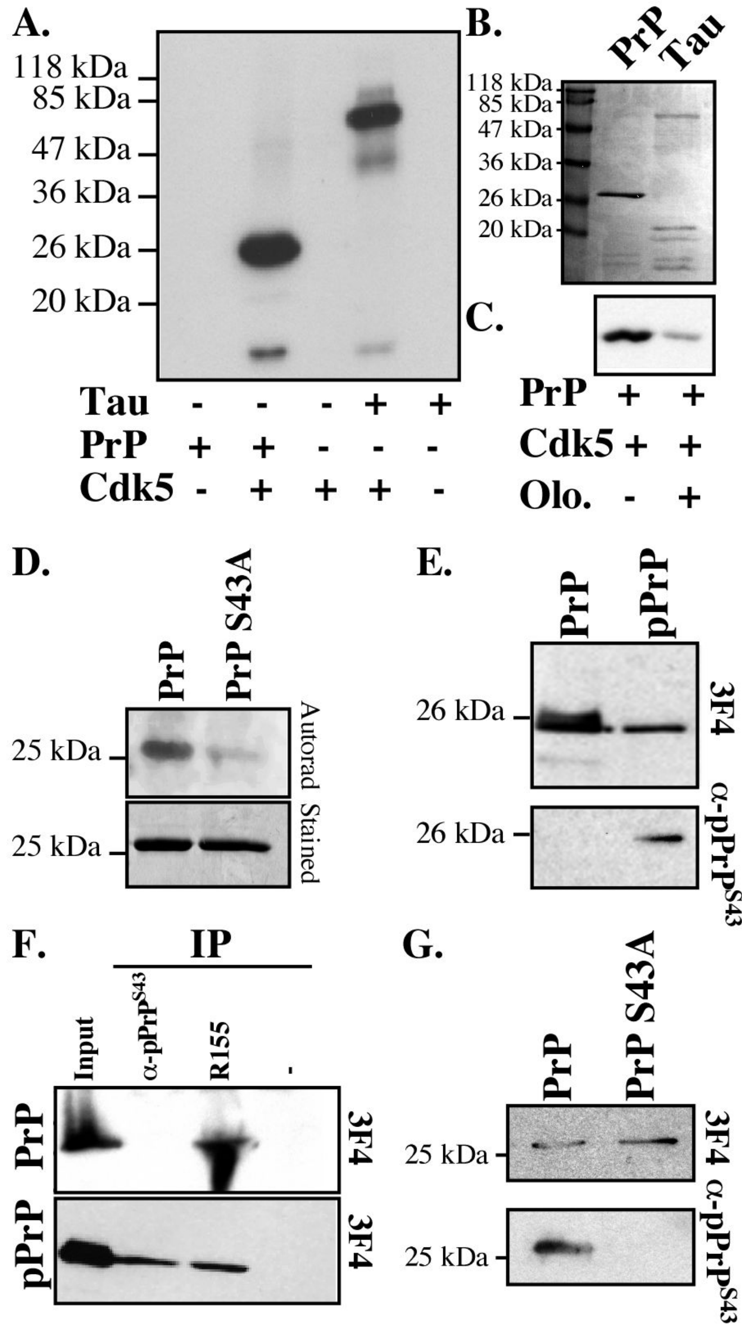

Figure 1. Cdk5-phosphorylation of human $PrP_{23\text{-}231}$ at S43

A. Autoradiogram of Cdk5 *in vitro* kinase assay on $PrP_{23\text{-}231}$ or Tau protein. **B.** Coomassie blue stain of PrP and Tau protein. **C.** Autoradiogram of *in vitro* Cdk5 kinase assay on PrP in the absence or presence of olomoucine. **D.** Autoradiogram and Coomassie blue stain of *in vitro* Cdk5 kinase assay on PrP and PrP S43A. **E.** Western blot with anti-$pPrP^{S43}$ antiserum and anti-$PrP^{109\text{-}112}$ 3F4 antibody of 100 ng of non-phosphorylated PrP or 100 ng of Cdk5-phosphorylated PrP (pPrP). **F.** Western blot with 3F4 antibody of PrP and pPrP immunoprecipitated with anti-$pPrP^{S43}$ or anti-$PrP^{36\text{-}56}$ R155 antisera. **G.** Western blot with 3F4 and antibodies of Cdk5 kinase assay on PrP or PrP S43A.

NIH-PA Author Manuscript

NIH-PA Author Manuscript

NIH-PA Author Manuscript

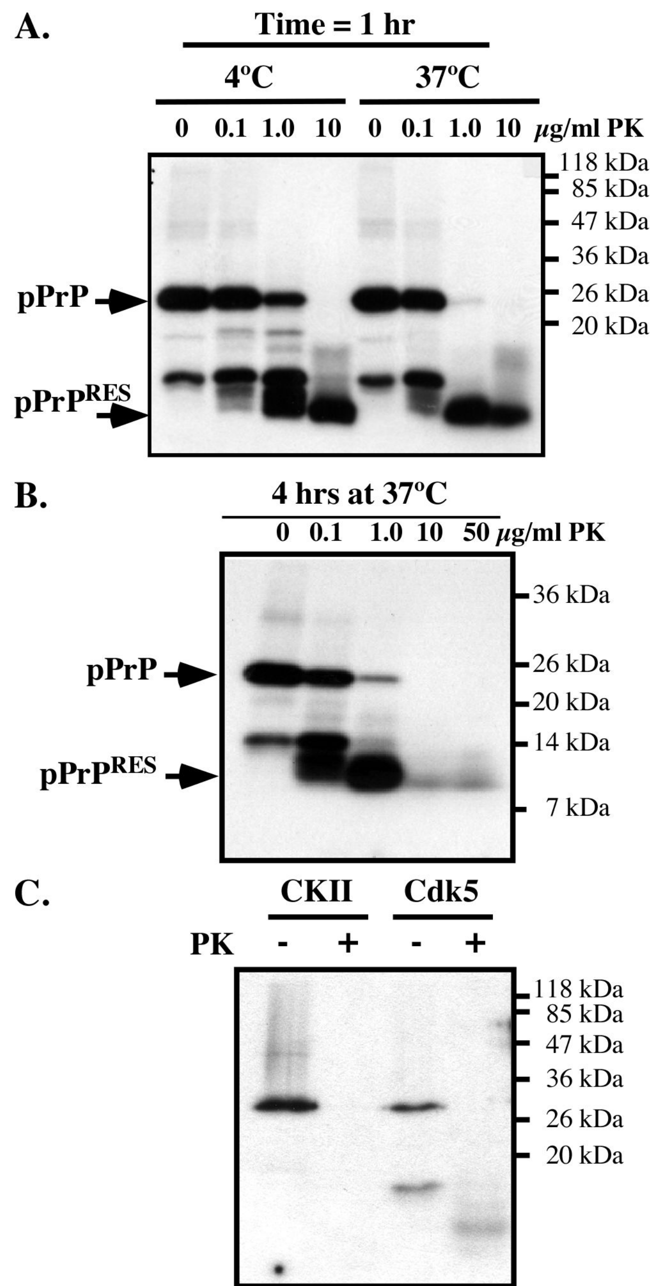

Figure 2. Cdk5-phosphorylated, but not CKII-phosphorylated PrP is resistant to PK

A. Autoradiogram of Cdk5-phosphorylated PrP incubated with 0-10 μg/ml of PK for 1 hour at 4°C or 37°C. **B.** Autoradiogram of Cdk5-phosphorylated PrP incubated with 0-50 μg/ml of PK for 4 hours at 37°C. **C.** Autoradiogram of Cdk5- or CKII-phosphorylated PrP incubated with 0 or10 μg/ml of PK for 1 hour at 37°C.

NIH-PA Author Manuscript
NIH-PA Author Manuscript
NIH-PA Author Manuscript

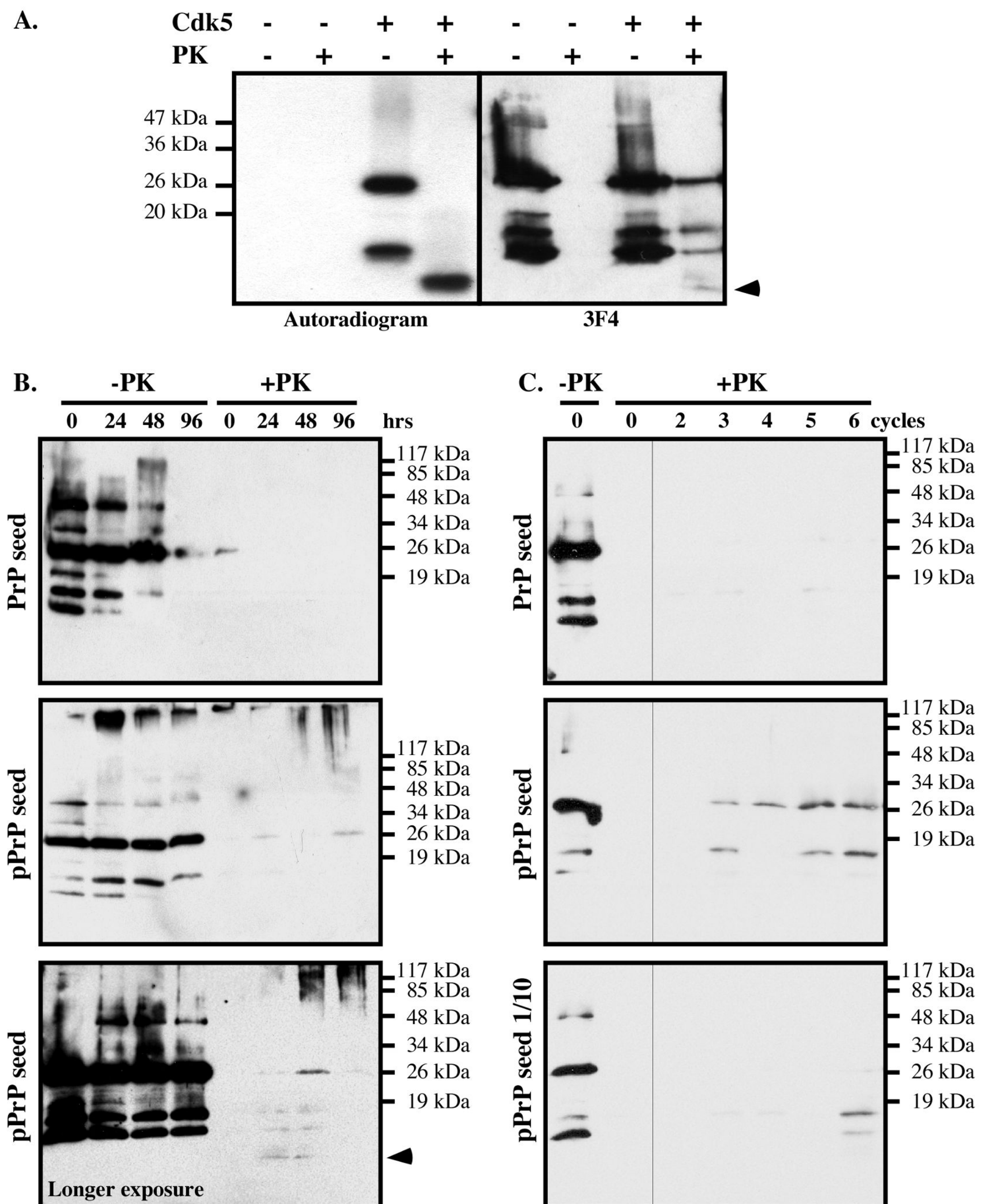

Figure 3. Cdk5-phosphorylated PrP induces the aggregation of non-phosphorylated PrP *in vitro*

A. Autoradiogram and western blot analysis with 3F4 antibody of non-phosphorylated or Cdk5-phosphorylated PrP treated with 10 μg/mL PK for 1 hr at 37°C. The arrow indicates the 10 kDa PrP^{RES} fragment detected on the autoradiogram or western blot. B. PrP western blot of non-phosphorylated PrP seeded with kinase assays performed with (pPrP) or without Cdk5, and incubated for the indicated time without (-PK) or with PK treatment (+PK). The lower panel shows a longer exposure of another pPrP seeded experiment revealing the 10 kDa PrP fragment in +PK. C. PrP western blot of non-phosphorylated PrP seeded with a 2 μl aliquot of the 96 hr time point (0 cycle) in 3B and incubated 24 hrs (cycle 1). Subsequent cycles represent samples where 2 μl at the end of the incubation period was added into fresh non-phosphorylated

NIH-PA Author Manuscript

NIH-PA Author Manuscript

NIH-PA Author Manuscript

PrP and incubated 24 hrs. The lower panel represents an original seed of 0.2 μl of the 96 hr time point in B.

NIH-PA Author Manuscript
NIH-PA Author Manuscript
NIH-PA Author Manuscript

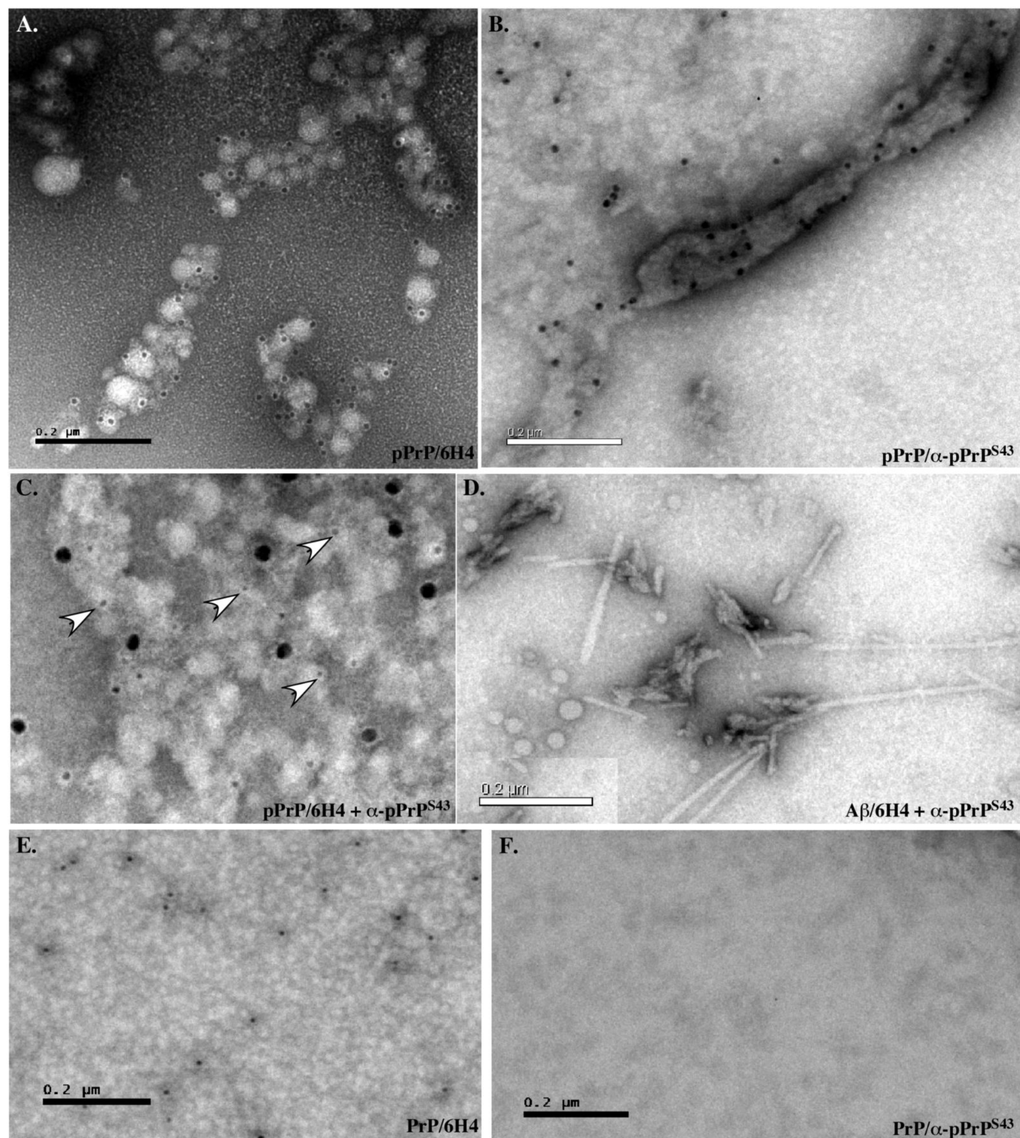

Figure 4. Cdk5-phosphorylated PrP forms aggregates

A-C. Immunostaining of pPrP with 6H4 (10 nm gold particle size) (**A**), anti-pPrP^{S43} (10 nm) (**B**) or both anti-pPrP^{S43} (18 nm) and 6H4 (5nm) antibodies (**C**). **D.** Control of fibrillar Aβ_{1-42} immunostaining with anti-pPrP^{S43} (10 nm). **E&F.** Immunostaining of non-phosphorylated PrP with 6H4 (10 nm) (**E**) and anti-pPrP^{S43} (10 nm) (**F**) antibodies.

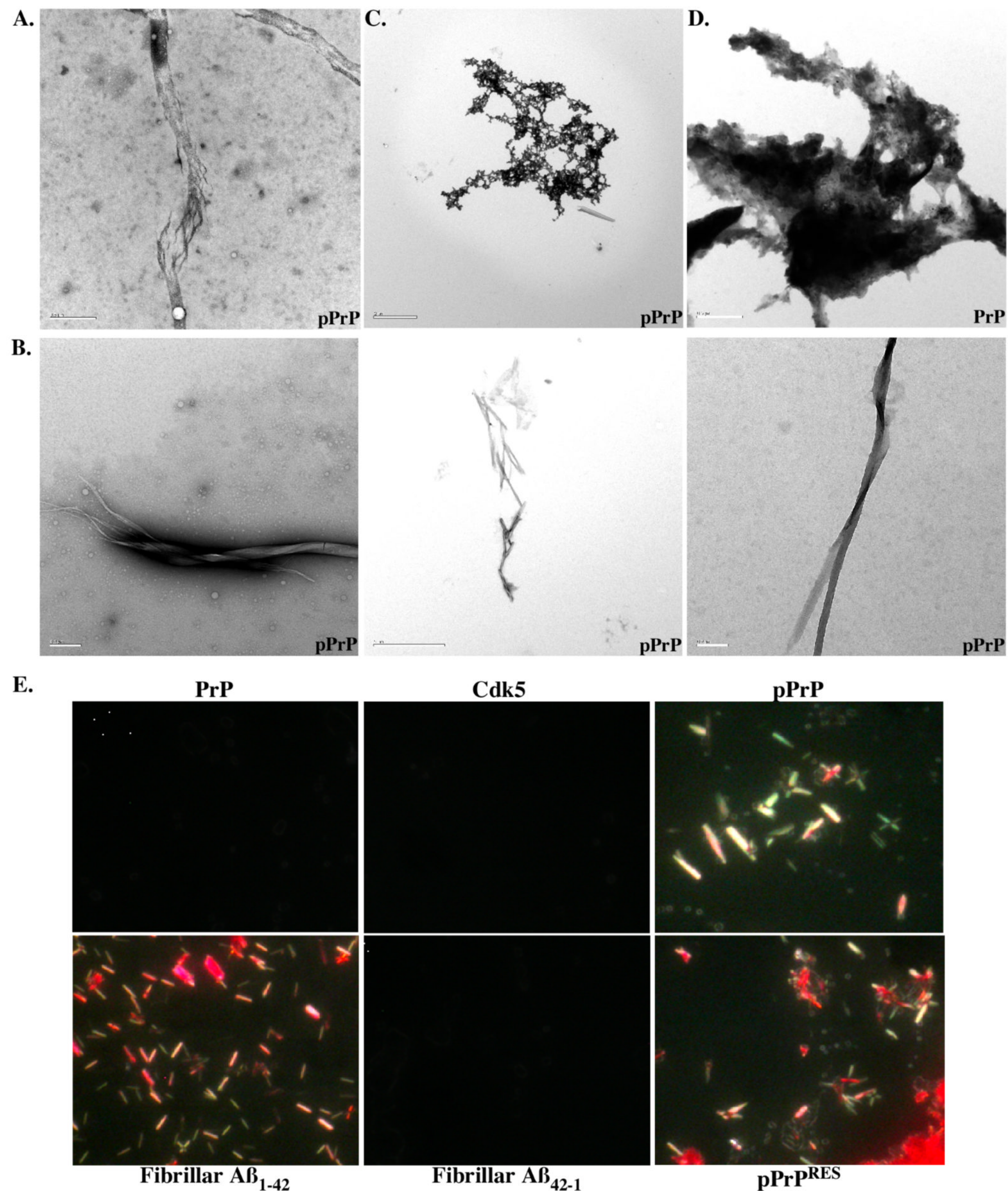

Figure 5. Cdk5-phosphorylated PrP forms fibrils

A. Electron micrograph of dialyzed Cdk5-phosphorylated PrP showing fibrillar-like structures. Bar=0.5 μm. **B.** Fibrils detected in pPrP after a 16 day incubation at 37°C. Bar=0.2 μm for left and right panels and 2 μm for middle panel. **C.** Compact structure of pPrP after a 16 day incubation at 37°C. Bar = 2 μm. **D.** Amorphous appearance of non-phosphorylated PrP after a 16 day incubation at 37°C. Bar= 0.5 μm. **E.** Congo Red staining of dialyzed PrP, Cdk5 alone, dk5-phosphorylated PrP (pPrP), PK digested pPrP ($pPrP^{RES}$), fibrillar $A\beta_{1-42}$ and $A\beta_{42-1}$. Pictures were taken under polarized light microscopy.

NIH-PA Author Manuscript NIH-PA Author Manuscript NIH-PA Author Manuscript

NIH-PA Author Manuscript

NIH-PA Author Manuscript

NIH-PA Author Manuscript

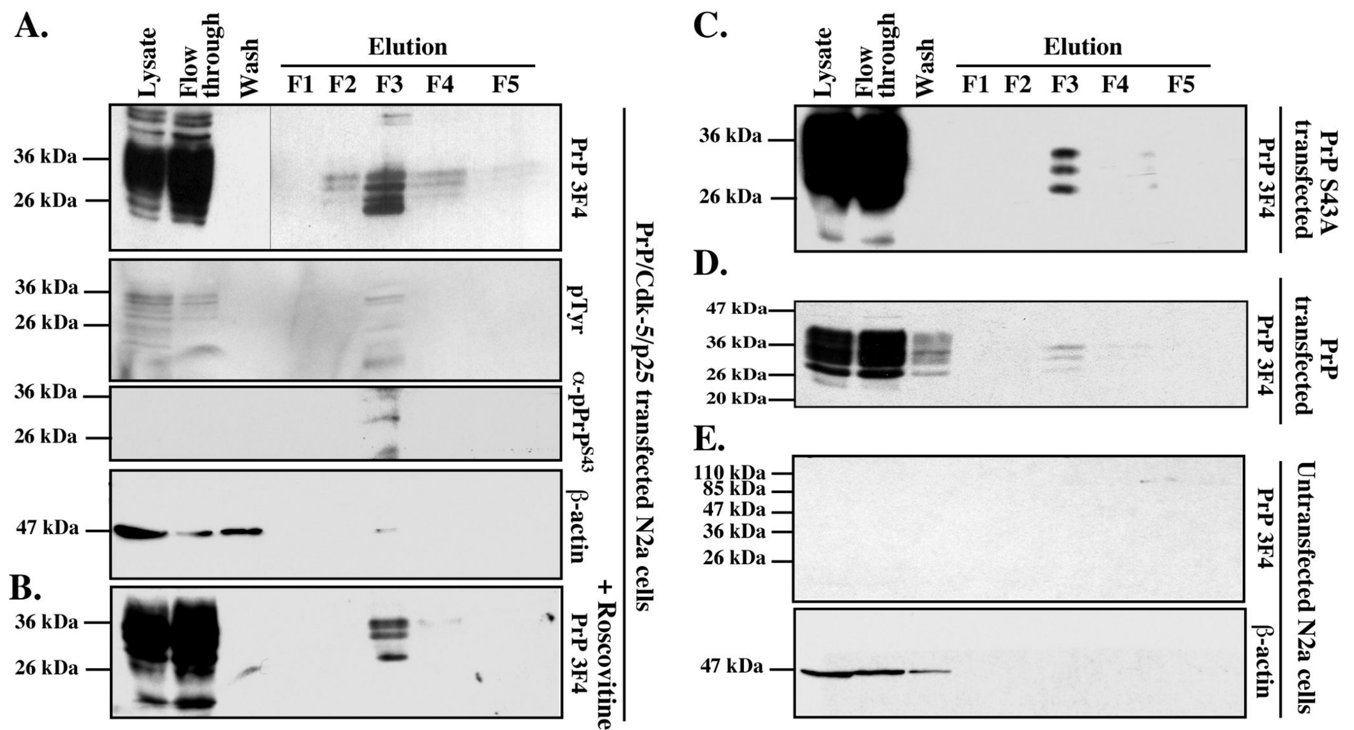

Figure 6. Purification of phosphorylated PrP from PrP/Cdk5/p25 co-transfected N2a cells protein extracts

A-D. Western blot analyses with 3F4, phospho-tyrosine (pTyr), anti-pPrP^{S43} and β-actin on phospho-column fractionated proteins from PrP/Cdk5/p25 co-transfected N2a cells (**A**), roscovitine-treated PrP/Cdk5/p25 co-transfected N2a cells (**B**), PrP S43A/Cdk5/p25 co-transfected N2a cells (**C**), PrP-transfected N2a (**D**), or untransfected N2a cells (**E**).

NIH-PA Author Manuscript
NIH-PA Author Manuscript
NIH-PA Author Manuscript

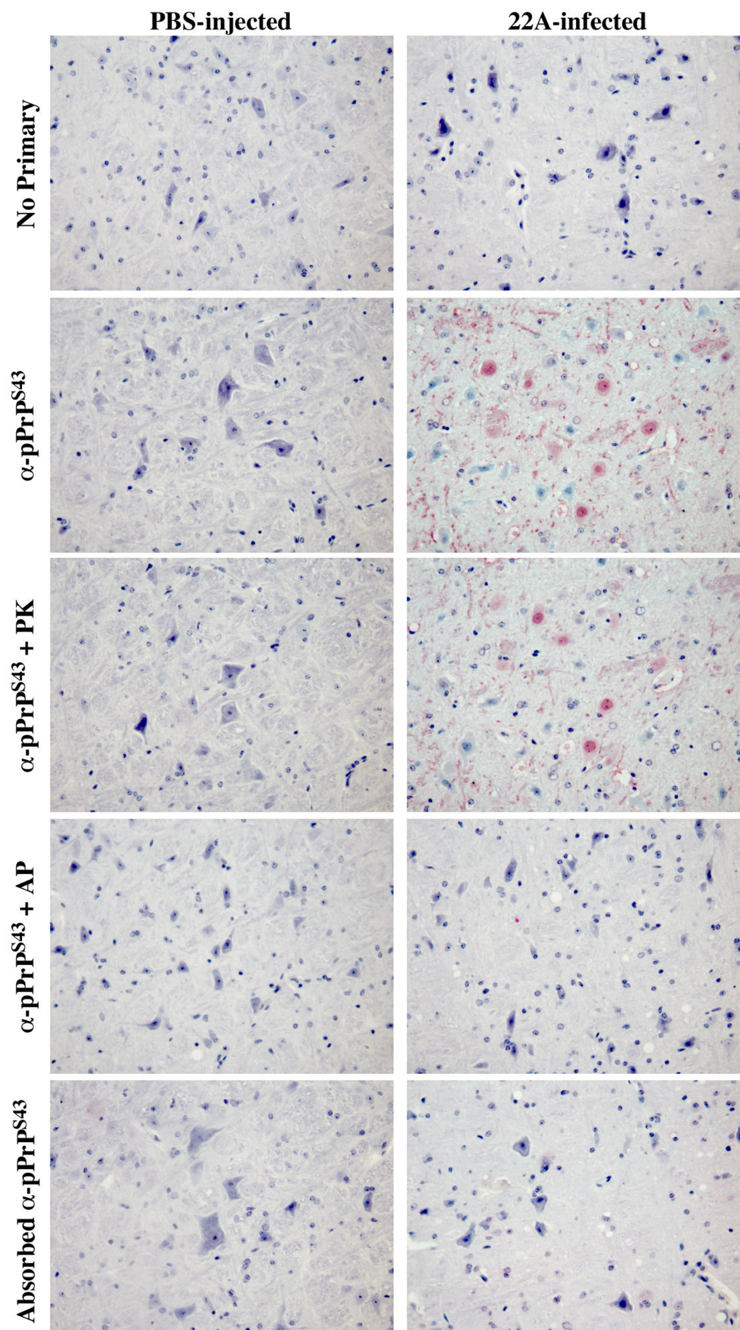

Figure 7. Immunohistological staining of control PBS- and 22A scrapie-infected mice brains

Micrographs of control PBS-injected or 22A-infected mice brain tissue sections of the medulla untreated (no primary, anti-pPrP^{S43}, adsorbed anti-pPrP^{S43}), pre-treated with PK (anti-pPrP^{S43}+PK), or pre-treated with alkaline phosphatase (anti-pPrP^{S43} +AP) with anti-pPrP^{S43}, no primary antiserum, or adsorbed anti-pPrP^{S43}.

NIH-PA Author Manuscript

NIH-PA Author Manuscript

NIH-PA Author Manuscript

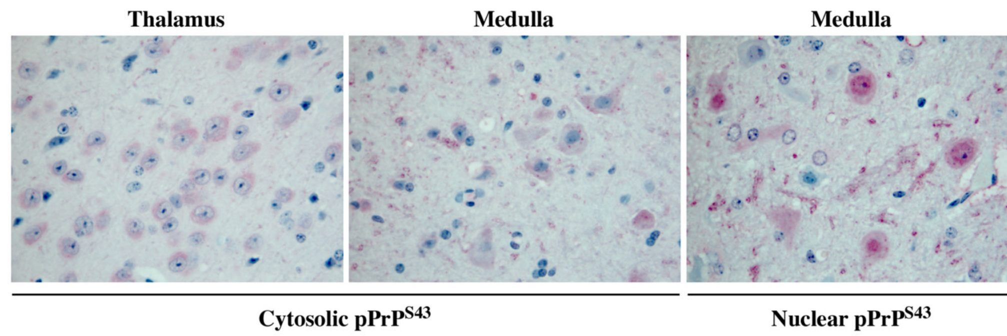

Figure 8. Cytosolic and nuclear pPrP^{S43} staining of 22A scrapie-infected mice brains

Higher magnification of micrographs of 22A-infected mice brain tissue sections from the thalamus or the medulla immunostained with anti-PrP^{S43}.

NIH-PA Author Manuscript NIH-PA Author Manuscript NIH-PA Author Manuscript

Table I

Conservation of phosphorylation motifs in PrP amongst various species

Mammalian species examined are human, guar, macaque, kudu, bison, rhesus monkey, baboon, mink, rabbit, camel, rat, nilgai, sheep, mouse, hamster, cattle and cat. Human Doppel was also included. The phosphorylation sites were identified with NetPhos 2.0 Server in EXPASY and had significant scores except the last SP motif(*), which has low predictability for phosphorylation.

Putative motif	Phospho AA	Mammals	Chicken	Turtle	Doppel
PGQ**SP**GGN	S43	All	RQ	SN	-
IHFG**S**DYED	S143	Only in human, bovine and bison	S	R	A
FGSD**Y**EDRY	Y145	W in rat, mouse and hamster	D	E	-
YEDR**Y**YREN	Y149	All	WW	WW	YY
PMDE**Y**SNQN	Y169	All	-	R	A
HTVT**T**TTKG	T191	All	P	P	F
TVTT**T**TKGE	T192	All	A	N	Q
VTTT**T**KGEN	T193	All	A	E	K
YQRG**S**SMVL	S230	All except rabbit	S	S	A
QRGS**S**MVLF	S231	All except rabbit	G	G	G
VLFS**SP**PVI*	S237	All	AD	DP	HQ